Journal Name

ARTICLE TYPE

Cite this: DOI: 00.0000/xxxxxxxxxx

Supplementary Material: Quantitative electrostatic force tomography for virus capsids in interaction with an approaching nanoscale probe†

Christopher D. Cooper[a,b], Ian Addison-Smith[a] and Horacio V. Guzman*[c,d]

Received Date
Accepted Date

DOI: 00.0000/xxxxxxxxxx

Poisson-Boltzmann solver

The Poisson-Boltzmann model in Eq. (1) of the main text can be decomposed as a system of two partial differential equations with constant field coefficients, coupled at the molecular surface. This is,

$$\begin{aligned}
\nabla^2\phi_m(\mathbf{r}) &= -\sum_k^{Nc}\frac{q_k}{\varepsilon_m}\delta(\mathbf{r},\mathbf{r}_k) \quad \mathbf{r}\in\Omega_m\\
\nabla^2\phi_w(\mathbf{r}) &= \kappa^2\phi_w(\mathbf{r}) \quad \mathbf{r}\in\Omega_w\\
\phi_m = \phi_w; \varepsilon_m\frac{\partial\phi_m}{\partial\mathbf{n}} &= \varepsilon_w\frac{\partial\phi_w}{\partial\mathbf{n}} \quad \mathbf{r}\in\Gamma_m\\
-\varepsilon_w\frac{\partial\phi_w}{\partial\mathbf{n}} &= \sigma_{tip} \quad \mathbf{r}\in\Gamma_t,
\end{aligned} \tag{1}$$

Using Green's second identity, we can write Eq. (1) as the following system of integral equations:

$$\begin{aligned}
\phi_m(\mathbf{r}) &= -K^{\Gamma_m}_{\mathbf{r},L}\left(\phi_{m,\Gamma_m}\right)+V^{\mathbf{r}}_{\Gamma_m,L}\left(\frac{\partial}{\partial\mathbf{n}}\phi_{m,\Gamma_m}\right)\\
&\quad+\frac{1}{\varepsilon_m}\sum_k^{N_c}\frac{q_k}{4\pi|\mathbf{r}-\mathbf{r}_k|} \quad \mathbf{r}\in\Omega_m\\
\phi_w(\mathbf{r}) &= K^{\mathbf{r}}_{\Gamma_m,Y}(\phi_{w,\Gamma_m})-V^{\mathbf{r}}_{\Gamma_m,Y}\left(\frac{\partial}{\partial\mathbf{n}}\phi_{w,\Gamma_1}\right)+K^{\mathbf{r}}_{\Gamma_2,Y}(\phi_{2,\Gamma_2})\\
&\quad-V^{\mathbf{r}}_{\Gamma_t,Y}\left(\frac{\partial}{\partial\mathbf{n}}\phi_{w,\Gamma_t}\right) \quad \mathbf{r}\in\Omega_2
\end{aligned} \tag{2}$$

where

$$\begin{aligned}
V^{\mathbf{r}}_{\Gamma_a}(\varphi) &= \oint_{\Gamma_a} G(\mathbf{r},\mathbf{r}')\varphi(\mathbf{r}')\mathrm{d}\mathbf{r}'\\
K^{\mathbf{r}}_{\Gamma_a}(\varphi) &= \oint_{\Gamma_a}\frac{\partial G}{\partial\mathbf{n}}(\mathbf{r},\mathbf{r}')\varphi(\mathbf{r}')\mathrm{d}\mathbf{r}'
\end{aligned} \tag{3}$$

are known as the single- and double- layer potentials, and

$$\begin{aligned}
G_L(\mathbf{r},\mathbf{r}') &= \frac{1}{4\pi|\mathbf{r}-\mathbf{r}'|}\\
G_Y(\mathbf{r},\mathbf{r}') &= \frac{e^{-\kappa|\mathbf{r}-\mathbf{r}'|}}{4\pi|\mathbf{r}-\mathbf{r}'|}
\end{aligned} \tag{4}$$

are the free-space Green's function of the Laplace and Yukawa (Poisson-Boltzmann) potentials. Evaluating Eq. (2) on $\Gamma_m\cup\Gamma_t$ gives

$$\begin{aligned}
&\frac{\phi_{m,\Gamma_m}}{2}+K^{\Gamma_m}_{\Gamma_m,L}\left(\phi_{m,\Gamma_m}\right)-V^{\Gamma_m}_{\Gamma_m,L}\left(\frac{\partial}{\partial n}\phi_{m,\Gamma_m}\right)\\
&\qquad=\frac{1}{\varepsilon_m}\sum_k^{N_c}\frac{q_k}{4\pi|r_{\Gamma_m}-r_k|}\\
&\frac{\phi_{w,\Gamma_1}}{2}-K^{\Gamma_m}_{\Gamma_m,Y}(\phi_{w,\Gamma_m})+V^{\Gamma_m}_{\Gamma_m,Y}\left(\frac{\partial}{\partial n}\phi_{w,\Gamma_m}\right)-K^{\Gamma_m}_{\Gamma_w,Y}(\phi_{w,\Gamma_w})\\
&\qquad+V^{\Gamma_m}_{\Gamma_w,Y}\left(\frac{\partial}{\partial n}\phi_{w,\Gamma_w}\right)=0\\
&\frac{\phi_{w,\Gamma_w}}{2}-K^{\Gamma_w}_{\Gamma_m,Y}(\phi_{w,\Gamma_m})+V^{\Gamma_w}_{\Gamma_m,Y}\left(\frac{\partial}{\partial n}\phi_{w,\Gamma_1}\right)-K^{\Gamma_w}_{\Gamma_w,Y}(\phi_{w,\Gamma_2})\\
&\qquad+V^{\Gamma_w}_{\Gamma_w,Y}\left(\frac{\partial}{\partial n}\phi_{w,\Gamma_w}\right)=0
\end{aligned} \tag{5}$$

[a] Department of Mechanical Engineering, Universidad Técnica Federico Santa María, 2390123 Valparaíso, Chile
[b] Centro Científico Tecnológico de Valparaíso (CCTVal), 2390123 Valparaíso, Chile.; E-mail: christopher.cooper@usm.cl
[c] Department of Theoretical Physics, Jožef Stefan Institute, Jamova 39, 1000 Ljubljana, Slovenia.; E-mail: horacio.guzman@ijs.si
[d] Departamento de Física Teórica de la Materia Condensada, Universidad Autónoma de Madrid, E-28049 Madrid, Spain.

which can be written in matrix form as

$$\begin{bmatrix} 1/2+K^{\Gamma_m}_{\Gamma_m,L} & -V^{\Gamma_m}_{\Gamma_m,L} & 0 \\ 1/2-K^{\Gamma_m}_{\Gamma_m,Y} & \frac{\varepsilon_m}{\varepsilon_w}V^{\Gamma_m}_{\Gamma_m,Y} & -K^{\Gamma_m}_{\Gamma_t,Y} \\ -K^{\Gamma_t}_{\Gamma_m,Y} & \frac{\varepsilon_m}{\varepsilon_w}V^{\Gamma_t}_{\Gamma_m,Y} & (1/2-K^{\Gamma_t}_{\Gamma_t,Y}) \end{bmatrix} \begin{bmatrix} \phi_m(r_{\Gamma_m}) \\ \frac{\partial}{\partial n}\phi_m(r_{\Gamma_m}) \\ \phi_w(r_{\Gamma_t}) \end{bmatrix} = \begin{bmatrix} \frac{1}{\varepsilon_m}\sum_k^{N_c}\frac{q_k}{4\pi|r_{\Gamma_1}-r_k|} \\ V^{\Gamma_m}_{\Gamma_t,Y}\left(\frac{\sigma_{tip}}{\varepsilon_w}\right) \\ V^{\Gamma_t}_{\Gamma_t,Y}\left(\frac{\sigma_{tip}}{\varepsilon_w}\right) \end{bmatrix} \quad (6)$$

We solve the system in Eq. (6) with the Poisson-Boltzmann solver PyGBe[1,2]. PyGBe is an implementation of a collocation-based boundary element method, which assumes a piece-wise constant distribution of ϕ and $\partial\phi/\partial\mathbf{n}$ on a triangulated approximation of the surfaces of the macromolecule and tip. The average simulation time was ∼3 hours per tip distance, performed on a GPU Tesla V100.

Details on the derivation of the electrostatics forces with Poisson-Boltzmann

The total electrostatic free energy of a dielectric cavity with point charges, inside a continuum medium can be written as[3]

$$G = \int_\Omega \left\{ \rho_f\phi - \frac{\varepsilon(x)}{2}|\nabla\phi|^2 - \frac{1}{2}\varepsilon\kappa^2\phi^2\lambda \right\} d\Omega, \quad (7)$$

where the first term is the energy of the point charges, the second term is the electrostatic stress, and the third one is the excess osmotic pressure. Eq. (7) is valid for the linearized Poisson-Boltzmann equation, and is equivalent to the well-known $G = \frac{1}{2}\int_\Omega \rho_f\phi d\Omega$. Taking the total variation of the free energy, we obtain[4]

$$\delta G = \int_\Omega \Big(\phi\delta\rho_f - \frac{1}{2}\nabla\phi\cdot\nabla\phi\delta\varepsilon - \frac{1}{2}\varepsilon\kappa^2\phi^2\delta\lambda + \rho_f\delta\phi - \varepsilon\nabla\phi\cdot\nabla(\delta\phi) - \varepsilon\kappa^2\phi\lambda\delta\phi \Big) d\Omega \quad (8)$$

Using the Poisson-Boltzmann equation, we can eliminate terms from Eq. (8), to get

$$\delta G = \int_\Omega \left(\phi\delta\rho_f - \frac{1}{2}\nabla\phi\cdot\nabla\phi\delta\varepsilon - \frac{1}{2}\varepsilon\kappa^2\phi^2\delta\lambda \right) \mathrm{d}\Omega \quad (9)$$

We can relate this equation with the virtual work theorem

$$-\delta G = \int_\Omega \mathbf{f}(r)\cdot\mathbf{s}(r)\mathrm{d}\Omega$$

to identify the force per unit volume f

$$\mathbf{f} = \rho_f\mathbf{E} - \frac{1}{2}\mathbf{E}^2\nabla\varepsilon - \frac{1}{2}\varepsilon\kappa^2\phi^2\nabla\lambda \quad (10)$$

The first term in Eq. (10) is the force due the charges in the solute, which we evaluate directly

$$\mathbf{F}_{\mathrm{qf}} = \int_\Omega \rho_f\mathbf{E}d\Omega = -\sum_k q_k\nabla\phi(\mathbf{r_k})$$

The two other terms of Eq. (10) require more work. Using the divergence theorem, we can identify a stress-tensor-type expression to calculate the forces[5]

$$\int \mathbf{f}d\Omega = \int \nabla\cdot\mathbf{P}d\Omega = \oint \mathbf{P}\cdot\mathbf{n}d\Gamma$$

This corresponds to the Maxwell tensor, plus a term that accounts for salt ions:

$$P_{ij} = \varepsilon E_iE_j - \frac{1}{2}\varepsilon E^2\delta_{ij} - \frac{1}{2}\varepsilon\kappa^2\phi^2\delta_{ij}.$$

In the force per unit volume f of Eq. (10), the force due to the dielectric jump is non zero on the molecular surface only. We can then equate this term to the jump of the Maxwell tensor across the molecular surface, as[6]:

$$\begin{aligned} \mathbf{f}_{db} &= (\mathbf{P}_o - \mathbf{P}_i)_{\mathrm{Maxwell}}\cdot\mathbf{n} \\ &= \left[\left(\varepsilon E_iE_j - \frac{1}{2}\varepsilon E^2\delta_{ij} \right)_o - \left(\varepsilon E_iE_j - \frac{1}{2}\varepsilon E^2\delta_{ij} \right)_i \right]\cdot\mathbf{n} \\ &= -\frac{1}{2}(\varepsilon_o - \varepsilon_i)(\mathbf{E}_o\cdot\mathbf{E}_i) \end{aligned}$$

allowing us to write:

$$\mathbf{F}_{\mathrm{db}} = -\int_\Omega \frac{1}{2}\mathbf{E}^2\nabla\varepsilon d\Omega = -\int_{\Gamma_m}\frac{1}{2}(\varepsilon_w - \varepsilon_m)(\mathbf{E}_w\cdot\mathbf{E}_m)\mathbf{n}d\Gamma_m$$

Finally, to obtain the third term, we recall the Maxwell tensor and apply the divergence theorem to obtain the force

$$\mathbf{F}_{\mathrm{ib}} = -\int_\Omega \frac{1}{2}\varepsilon\kappa^2\phi^2\nabla\lambda d\Omega = -\int_{\Gamma_m}\frac{1}{2}\kappa^2\varepsilon_w\phi^2\mathbf{n}d\Gamma_m$$

Details on the force contribution of different amino acids

Fig. S1(a) is a close-up view of Fig. 3 (a) of the main text, which allows us to see in more detail the distribution of the force on the charges. Even though the highest force is on the rightmost region, there is an important penetration of the influence of the tip, and we see high-force atoms deeply buried in the capsid. Comparing Figs. S1(a) and (b) shows the influence of salt concentration in the solvent, as it decreases the penetration of electrostatics in the capsid.

Fig. S2 is helpful to understand the non monotonic behavior of the force in Fig. 4(a) of the main text. This is explained by the difference in number of atoms in each slice, and dividing by the atom count, we recover a monotonic behavior. Again, comparing S2(a) and (b) is evidence that the shielding of the free ions decrease the influence of electrostatics.

Table S1 shows the top 10 atoms that feel most force for the conical tip in a 20 mM ionic solvent. Even though in Fig. 4 of the main text we see that the amino acid that contributed the most to the force is LYS, the atoms with highest force correspond to GLU. This is because all of these atoms belong to the right-most slice, where GLU dominates the force. It is interesting to see that the force on a single atom is of the order of the force over the whole

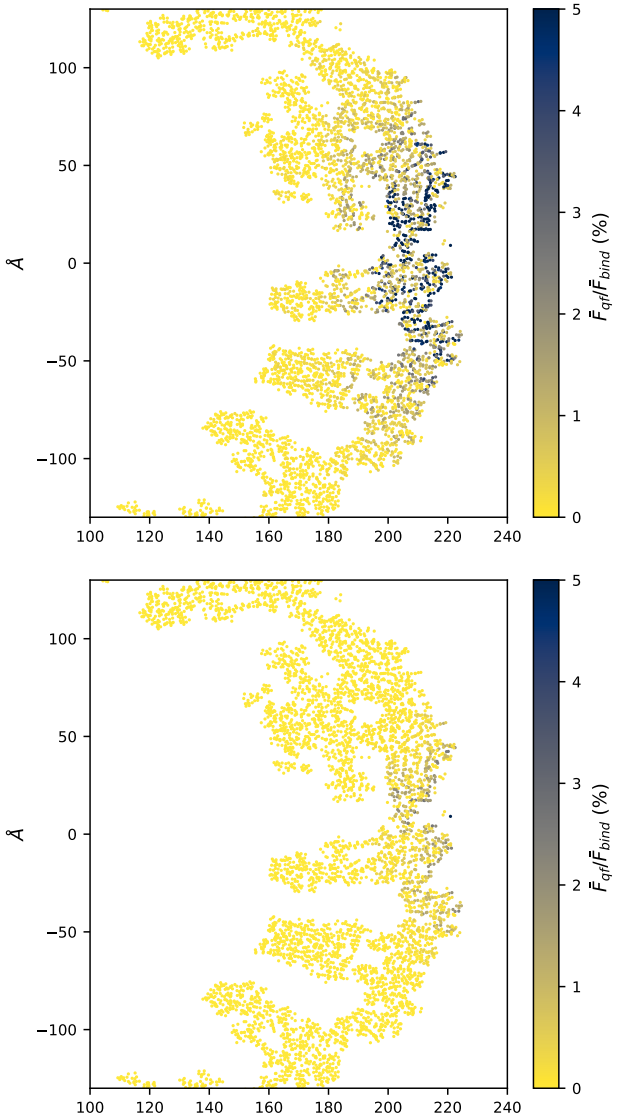

Fig. S1 Close-up view of Fig. 3a of the main text (top) and S4 (bottom).

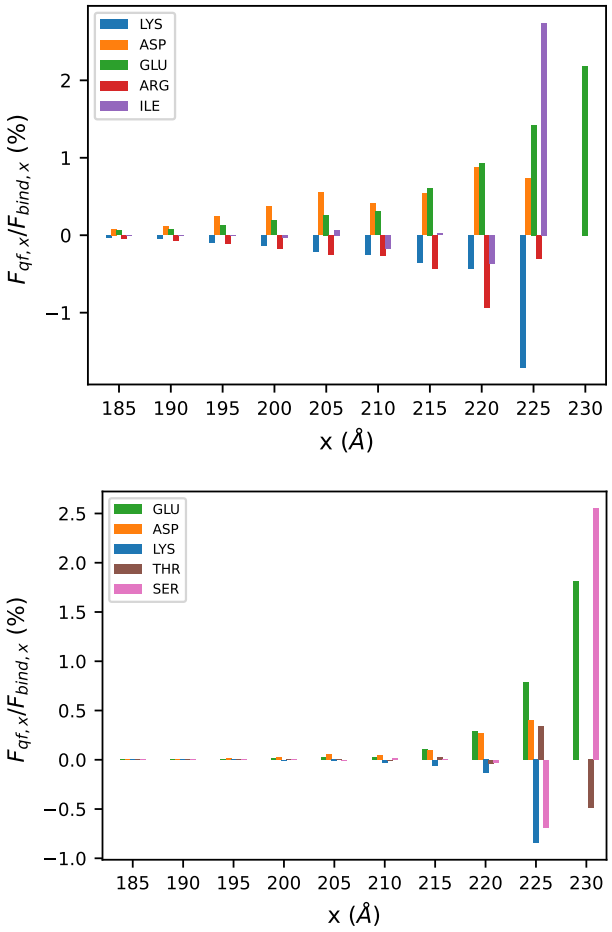

Fig. S2 Average force per unit atom with 20 mM (top) and 150 mM (bottom).

structure, indicating large cancellation of forces. The results in Table S3 helps us understand the source of the large opposite forces, which are aligned with the net charges of the atoms of the different amino acids.

Table S2 corresponds to the values plotted in Fig. 4(c) of the main text. We clearly observe that at the apex of the virus capsid only 3 of the 5 most sensitive amino acids are located within the 5Åslices.

Furthermore, Table S3 corresponds to the values plotted in Fig. 4b of the main text. As pointed out within the main text we can see how ILE changes polarities as a function of the slices, i.e. the charges of atoms within the slices of these 2 amino acids.

Results for higher salt concentration

The results of this section study the effect of salt concentration. We performed the same analysis as the case with 20 mM of salt discussed in the main text, this time, with 150 mM, and present the results in Figs. S3, S4, and S5.

Force mag. [pN]	Atom name	Residue name	Atom x-position
2.503	OE1	370GLU	232.019
1.996	CD	370GLU	231.158
1.846	OE2	370GLU	230.727
1.209	ND2	371ASN	227.684
1.161	OG1	335THR	228.893
1.151	OE2	367GLU	229.269
1.129	OG	368SER	227.850
1.115	OE1	367GLU	229.823
1.110	OG1	335THR	230.714
1.109	OE1	370GLU	230.906

Table S1 Top 10 atoms that are subject to the largest force when $d = 2$ Åfor a conical tip in a solvent with 20 mM of salt. All atoms shown here belong to the chain labelled as C in the PDB file.

Slice center	LYS	ASP	GLU	ARG	ILE
200	1201	600	684	796	621
205	899	278	650	753	563
210	813	324	559	527	354
215	632	236	359	240	192
220	246	150	89	50	50
225	44	45	70	3	5
230	0	0	36	0	0

Table S2 Number of atoms per amino acid in slices of 5 Å, moving along the x direction.

Slice center	LYS	ASP	GLU	ARG	ILE
200	53.74	-42.28	-47.67	3.35	6.06
205	39.85	-23.69	-35.98	3.09	-4.22
210	37.11	-26.03	-37.19	2.49	5.23
215	30.30	-17.75	-30.61	1.05	-0.78
220	12.40	-13.99	-7.57	3.65	1.04
225	4.74	-3.16	-5.19	0.03	-0.62
230	0	0	-2.42	0.00	0.00

Table S3 Net charge per amino acid in slices of 5 Å, moving along the x direction.

As expected, higher salt increases the shielding effect, and forces are lower (see Fig. S3). This has an impact on the penetration of the electrostatics in the capsid, which is evident comparing the top and bottom pane of Fig. S1, and looking at Fig. S4. Also, Fig. S5 shows a monotonic charge distribution, which is different from Fig. 4(a) of the main text. Another important change is the list of amino acids with highest force, which in this case is GLU, ASP, LYS, THR, and SER (in that order), whereas with 20 mM this was LYS, ASP, GLU, ARG, and ILE. This is evidence that the shielding effect is not homogeneous among atoms, and highlights the need of a detailed description of the capsid.

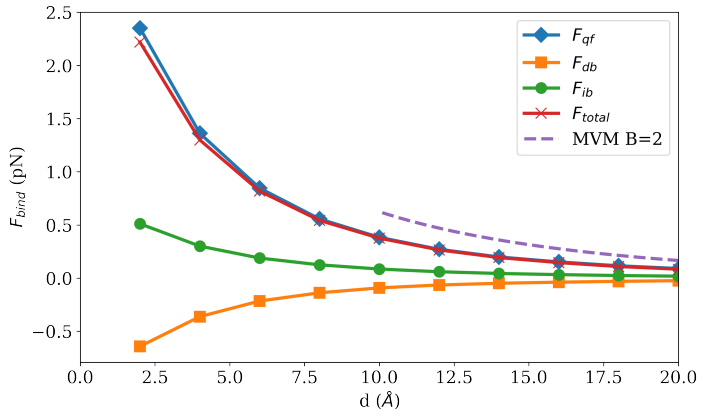

Fig. S3 Components of the electrostatic force for a conical tip in a 150 mM salt solution. The segmented line corresponds to the total force computed with a semi-empirical approach[7] on the minute virus of mice.

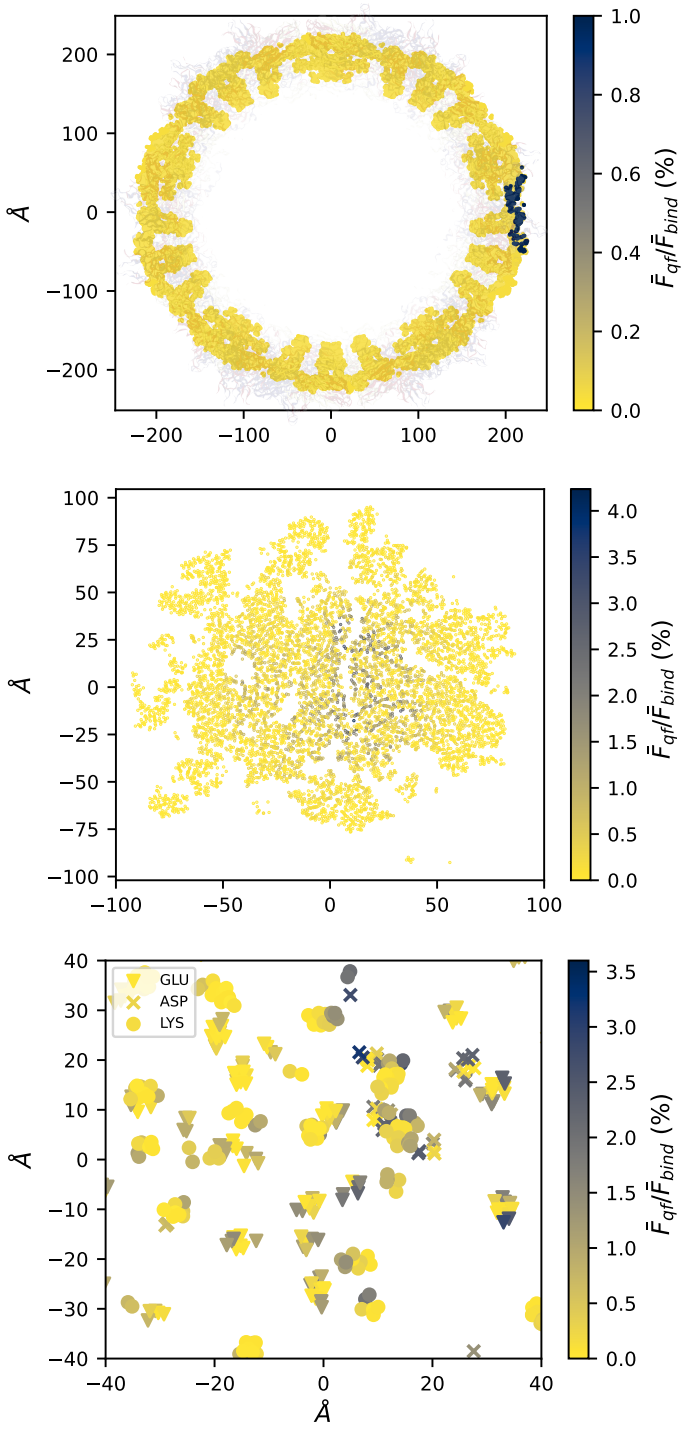

Fig. S4 Relative magnitude of $\mathbf{F}_{qf}$ on atoms located in a 5 Å slice centered at the z=0 Å plane (top) and the x=210 Å plane (middle). The bottom pane is a close-up view of the middle pane, and identifies atoms that belong to the amino acids with highest force in that plane (GLU, ASP, and LYS). In these plots, the distance between the molecular surface of the capsid and the conical tip was d=2 Å, and the solvent had 150 mM of salt.

Results for a spherical tip with high salt concentration

To study the impact of geometry in the capsid-tip interation, we performed the same set of computational experiments consider-

ing a spherical tip. In this case, we considered the same radius than the point of the tip used in the main text (r= 15 nm), a surface charge of $\sigma_{tip} = -2.5$ C/m^2, and the solvent had a salt concentration of 150 mM. We understand this high salinity shields the electrostatic component, and van der Waals effects become more important, however, these results are still interesting to study the role of free ions in the electrostatic component of the force.

Fig. S6 shows that the electrostatic force drops in comparison to lower salt cases, which is an expected behavior. It is interesting to note that at this special case of 150 mM, the boundary forces ($\mathbf{F}_{ib}$ and $\mathbf{F}_{db}$) cancel out almost exactly. More details are given by Figs S7 and S8, that show that at higher salt, the locality of the electrostatic force is more evident, as the penetration of the force is smaller. We can also see that the amino acids that contribute the most to the force are different with respect to the cases with lower salt. This can be explained by the fact that the change in the shielding effect does not affect all atoms homogeneously, as it depends on the amount of solvent between the tip and each individual atom.

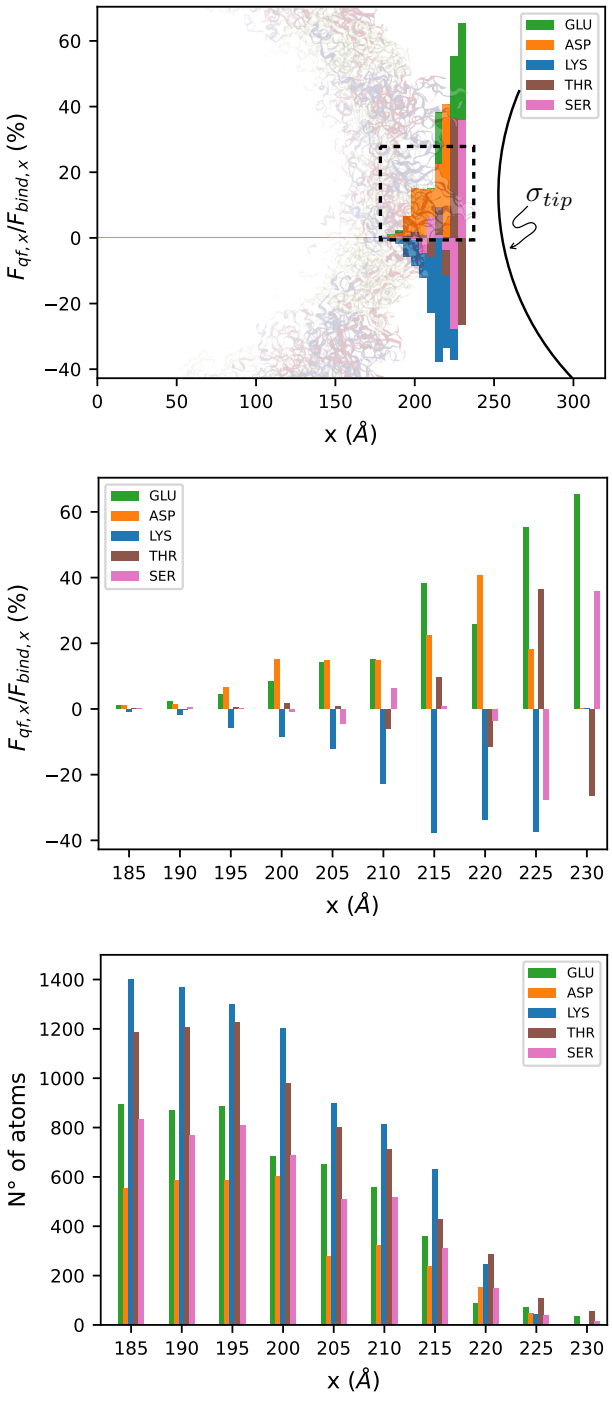

Fig. S5 The top pane shows the x-component of the interaction force (normalized) on atoms that belong to the 5 amino acids that contribute the most to the force (GLU, ASP, LYS, THR, and SER, in that order) on 5 Å-thick slices. As reference, we show the Zika capsid structure in the background, and the AFM tip, which is placed 2 Å away. The dotted line indicates the region of the close-up view in the middle and bottom panes, which correspond to the normalized force (x-component) and number of atoms, respectively.

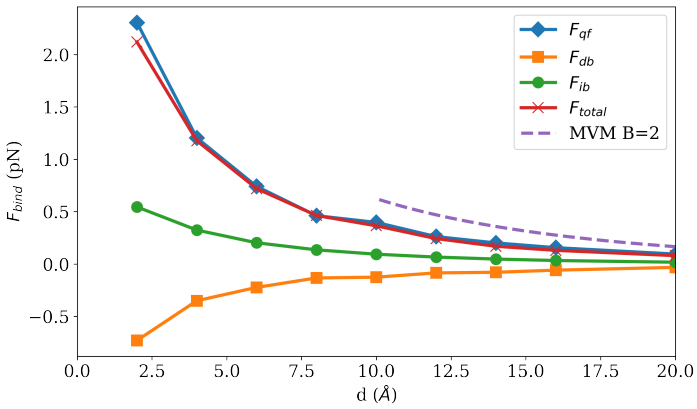

Fig. S6 Components of the electrostatic force for a spherical tip in a solvent with 150 mM of salt. The segmented line corresponds to the total force computed with a semi-empirical approach[7] on the minute virus of mice.

References

1 C. D. Cooper, J. P. Bardhan and L. A. Barba, *Comput. Phys. Commun.*, 2014, **185**, 720–729.

2 C. D. Cooper, N. C. Clementi, G. Forsyth and L. A. Barba, *The Journal of Open Source Software*, 2016, **1**, year.

3 K. A. Sharp and B. Honig, *Journal of Physical Chemistry*, 1990, **94**, 7684–7692.

4 M. K. Gilson, M. E. Davis, B. A. Luty and J. A. McCammon, *Journal of Physical Chemistry*, 1993, **97**, 3591–3600.

5 L. Xiao, Q. Cai, X. Ye, J. Wang and R. Luo, *Journal of Chemical Physics*, 2013, **139**, year.

6 Q. Cai, X. Ye and R. Luo, *Physical Chemistry Chemical Physics*, 2012, **14**, 15917–15925.

7 M. Hernando-Pérez, A. Cartagena-Rivera, A. L. Božič, P. J. Carrillo, C. San Martín, M. G. Mateu, A. Raman, R. Podgornik and P. De Pablo, *Nanoscale*, 2015, **7**, 17289–17298.

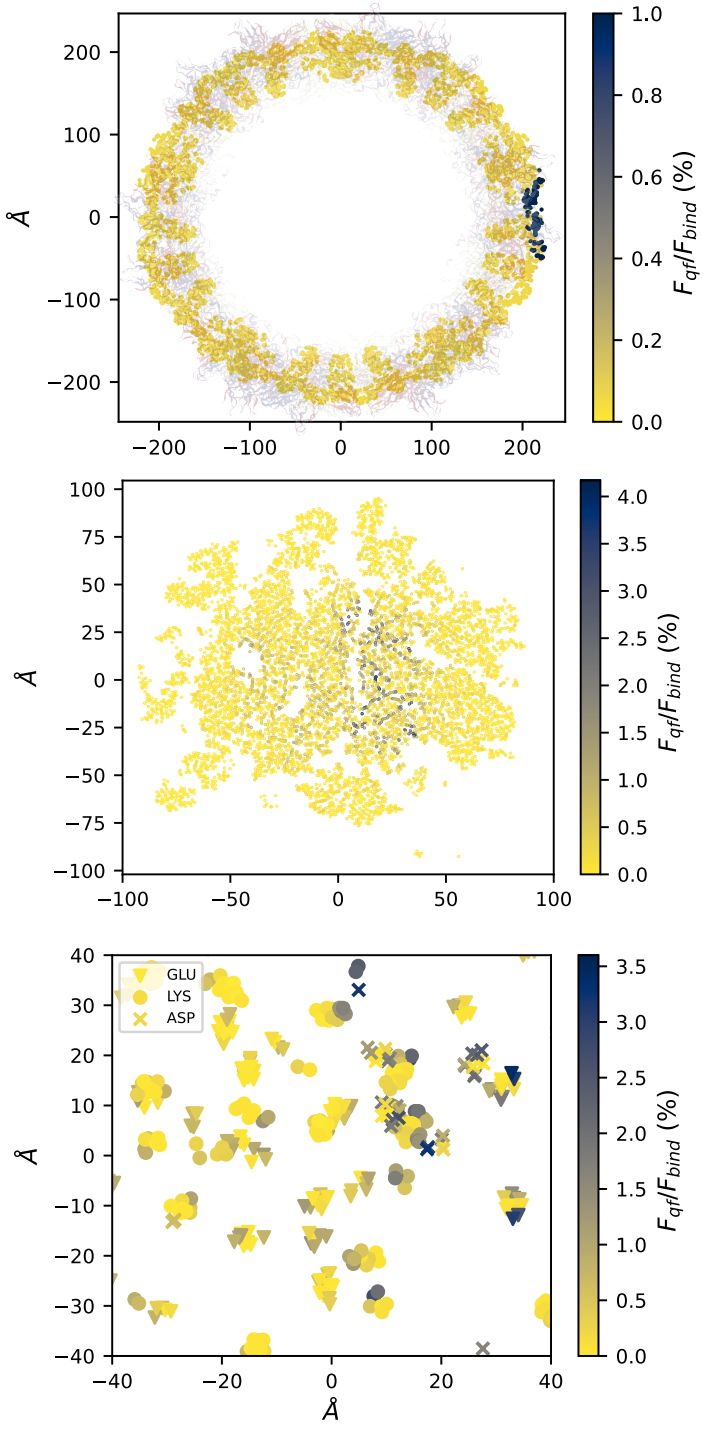

Fig. S7 Relative magnitude of $\mathbf{F}_{qf}$ on atoms located in a 5 Å slice centered at the z=0 Å plane (top) and the x=210 Å plane (middle) for a spherical tip in a solvent with 150 mM of salt. The bottom pane is a close-up view of the middle pane, and identifies atoms that belong to the amino acids with highest force in that plane (GLU, LYS, and ASP). In these plots, the distance between the molecular surface of the capsid and the tip was d=2 Å.

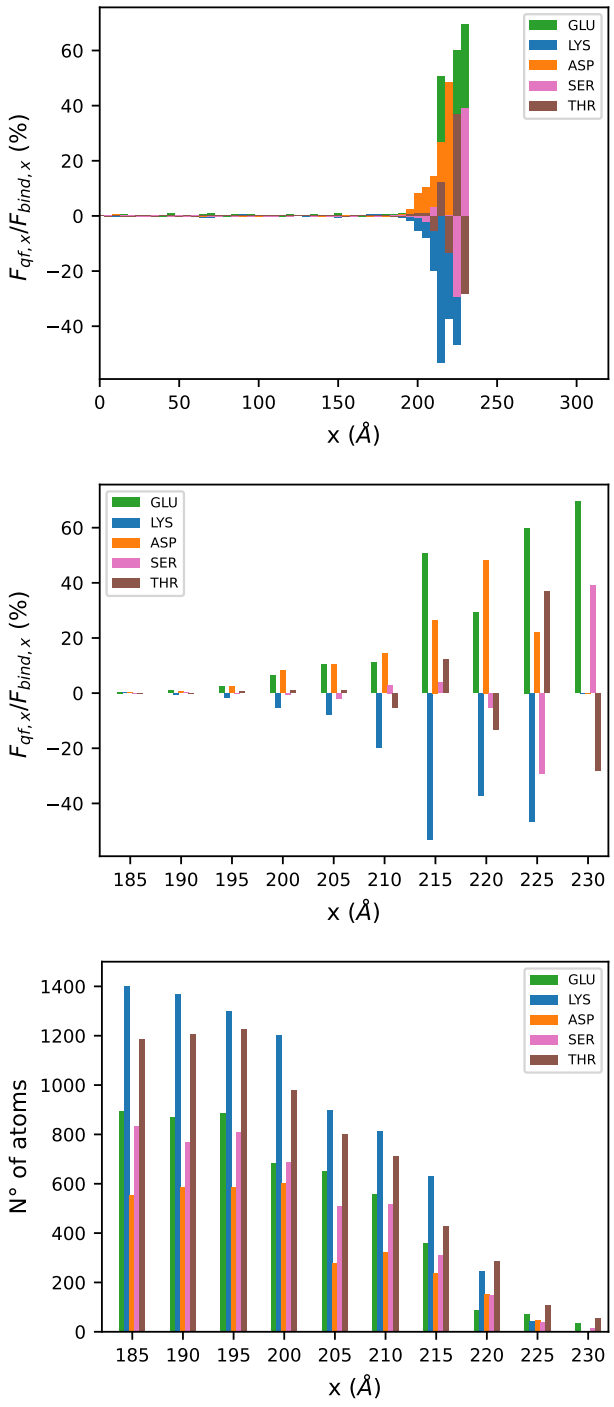

Fig. S8 The top pane shows the x-component of the interaction force (normalized) on atoms that belong to GLU, LYS, ASP, SER, and THR on 5 Å-thick slices for a spherical tip in a solvent with 150 mM of salt. As reference, we show the Zika capsid structure in the background, and the AFM tip, which is placed 2 Å away. The dotted line indicates the region of the close-up view in the middle and bottom panes, which correspond to the normalized force (x-component) and number of atoms, respectively.